Chemistry and kinetics of the GaAs oxidation by plasma anodization: An *in situ* real-time ellipsometric study

M. Losurdo, P. Capezzuto, and G. Bruno
Centro di Studio per la Chimica dei Plasmi, CNR, Dipartimento di Chimica, Università di Bari, via Orabona 4, 70126 Bari, Italy
(Received 31 March 1997)

In situ real-time ellipsometry is used to study the GaAs oxidation process by radio-frequency plasma anodization. The effect of the GaAs surface temperature, the bias potential applied to GaAs substrate, the crystallographic orientation, and UV-light irradiation on the chemistry and kinetics of GaAs oxidation are investigated. Oxide layers from tenths to hundreds of angstroms in thickness are grown at temperatures as low as 130 °C and bias voltages ranging between 5 and 50 V. The rate of oxidation is further increased by irradiation of the GaAs surface with UV light during plasma anodization. The role of the diffusion of oxidizing species and of the drift of gallium and arsenic ions on the oxidation kinetics is discussed and the UV photoenhancement effect is clarified. These plasma-grown GaAs oxide layers have a unique composition in that they are almost stoichiometric and contain As_2O_5 as the main arsenic oxide. [S0163-1829(97)05139-4]

I. INTRODUCTION

Since the 1960s a strong effort has been devoted to develop a metal-oxide-semiconductor (MOS) technology based on III-V material similar to that of the Si/SiO_2 system. However, the chemistry between GaAs and its native oxide does not lead to a chemically stable and defect-free interface compatible with MOS device operation. The widely investigated thermal[1,2] and anodic[3,4] oxidation of GaAs gives nonstoichiometric and nonhomogeneous Ga_2O_3/As_2O_3 mixtures with free As collected at the oxide/GaAs interface. Thus, research of dry methods for low-temperature GaAs oxidation improving the quality of the GaAs oxide interface is still active. In this context, the optical excitation with visible or ultraviolet (UV) light of GaAs surfaces and the plasma anodization, by ECR (electron cyclotron resonance) or radio-frequency glow discharge, even though not really new, are still under investigation to develop a key technique to grow GaAs oxide layers with good electrical properties. The effect of UV-light irradiation has been investigated[5–7] on GaAs surfaces exposed to oxygen gas at room temperature to grow very thin oxide layers (<30 Å). Although a photoenhancement of the GaAs oxidation rate has been reported, the actual mechanism for the rate enhancement in photon-assisted oxidation is as yet not defined. Also, many papers have been published over the years on the interaction of oxygen plasmas with GaAs surfaces, and most of the fundamentals of the plasma oxidation kinetics and chemistries have been already described in the 1980s by Sugano and co-workers,[8,9] and Chang and co-workers.[10–12] Furthermore, Theeten *et al.*[13] demonstrated the capability of ellipsometry to investigate *in situ* and in real time the plasma oxidation process and the properties of plasma-grown oxides. They concluded that ''the study on the oxidation of GaAs is by no means conclusive, there are still many facets that remain to be understood.'' Although much work has been produced in the past 20 years, the debate on the validity of GaAs plasma oxidation is still lively and open. There are still problems to be solved in making the GaAs plasma oxidation practically useful. In particular, questions regarding the initial oxidation region which determines the GaAs oxide interface quality, the species moving during oxidation, and the effect of UV-light irradiation on the plasma oxidation kinetics and chemistry are still without firm answers.

In this paper, we report on the combined effect of UV-light irradiation and of an external electric field on the rf plasma oxidation of GaAs. Particular emphasis is addressed to the investigation of the initial oxidation regime, i.e., the growth of the first 100 Å of oxide. *In situ* single wavelength ellipsometry (SWE) is used to investigate in real time the oxidation kinetics and spectroscopic ellipsometry (SE) allows us to evaluate the composition and morphology of the grown oxide. *Ex situ* x-ray photoelectron spectroscopy (XPS) is used to determine the chemical composition of the grown oxide layers.

II. EXPERIMENT

The remote plasma deposition apparatus used for the present study and described in Ref. 14, consists of a rf (13.56 MHz) plasma tube with external electrodes coupled to a stainless-steel metal-organic chemical-vapor deposition reactor equipped with a phase modulated ellipsometer (UVISEL-ISA-Jobin Yvon) for *in situ* measurements.

Single-crystal semi-insulating GaAs wafers with (100), (110), and (111)*A* crystallographic orientations were used as substrates. Before running oxidation, the substrates were cleaned *in situ* by exposing the surface, at $T=230$ °C, to a flux of hydrogen atoms of 5×10^{20} atoms/cm^2 sec produced by a remote hydrogen glow discharge according to the procedure reported in detail in Ref. 15. The GaAs surface was characterized by *in situ* spectroscopic ellipsometry, and an initial ellipsometric spectrum (spectrum b), acquired just prior to running oxygen plasma processing, is shown in Fig. 1 which shows a clean GaAs surface with a 25 Å-thick topmost layer of *c*-GaAs including 9% of voids. The void fraction simulates the void space present in the GaAs lattice, due to the selective removal of oxygen atoms, as well as the surface roughness arising from the plasma exposure and its

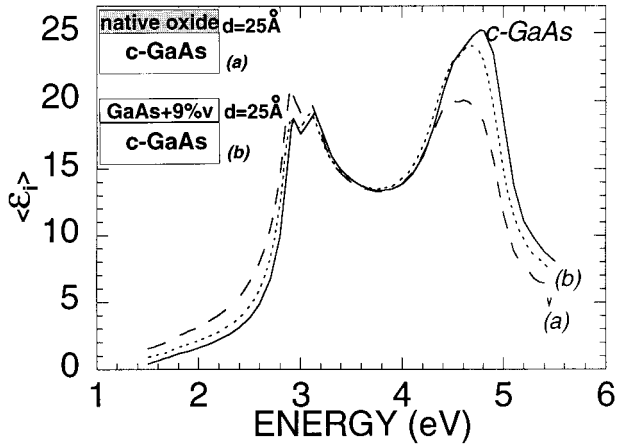

FIG. 1. Imaginary part of the pseudodielectric function $\langle \varepsilon_i \rangle$ of GaAs substrates (a) with native oxide and (b) after cleaning by hydrogen plasma; the reference *c*-GaAs database is also reported. The inset shows the best-fit BEMA models of the corresponding SE spectra.

validity has been discussed and demonstrated in Ref. 15. Thus, the red shift and lowering of the spectra (a) and (b) with respect to that of the *c*-GaAs reference are related to the presence of either a rough surface layer or an oxide layer. Moreover, the main advantage of the H-atom cleaning is linked to the removal of interfacial arsenic as AsH_3 from the GaAs/native oxide interface and simultaneous passivation of As-related defects.[16]

GaAs plasma oxidation was operated at a rf power of 100–300 W at a total pressure of 10^{-2}–10^{-1} mbar by feeding the plasma with a O_2:Ar=10 SCCM:2 SCCM mixture and at a substrate temperature ranging between 25–250 °C. (SCCM denotes cubic centimeter per minute at STP.) A dc bias potential from 0 to 70 V was applied to the GaAs surface during the plasma oxidation. The distance between the active plasma region and the GaAs substrate was 10 cm.

To investigate the effect of UV-light irradiation on the GaAs plasma oxidation kinetics, a high-pressure mercury arc lamp emitting mainly at 253.7 nm was used to irradiate the GaAs surfaces.

The chemical composition of the grown oxide film was characterized by *ex situ* angle-resolved X-ray photon emission spectroscopy (XPS) analysis. XPS measurements were performed with a Perkin-Elmer 5300 spectrometer using an unmonochromatized Mg $K\alpha$ (1253.6 eV) source. The O 1*s*, C 1*s*, Ga 3*d*, and As 3*d* photoelectron peaks were mainly investigated at take-off angles $\Theta = 15°$, 45°, 85°, corresponding to sampling depth of about 20, 60, and 80 Å, respectively. Au $4f_{7/2}$ [binding energy BE=83.9 eV] and Cu $2p_{3/2}$ (BE=932.7 eV) core levels of gold and copper standards were used to calibrate the binding energy scale. Shifts in energy of the XPS spectra due to electrical charging of the sample surface were corrected by fixing the C 1*s*, photoelectron peak from adventitious carbon on the surface at Be=284.6 eV. The average atomic composition of the oxide layers was evaluated from the O 1*s*, C 1*s*, Ga 3*d*, and As 3*d* peak areas by using a standard formalism for semiquantitative analysis and the sensitivity factors supplied by Perkin Elmer. Mixed Gaussian-Lorentzian curves were fitted to the spectra in order to obtain information on the gallium and arsenic bonding configurations in the oxide layer.

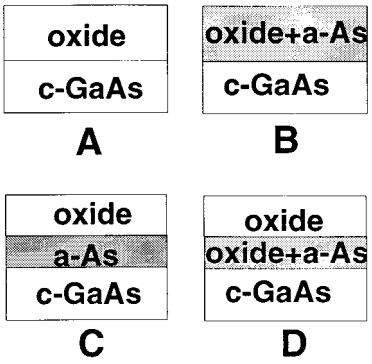

FIG. 2. Optical models considered for the fit of the experimental SWE and SE oxidation data.

Real-time single wavelength ellipsometry at the photon energy of 3.45 eV, which is insensitive to GaAs surface temperature variation, was used to monitor the oxidation kinetics. Ellipsometric spectra were acquired *in situ* in the energy range 1.5–5.5 eV and modeled using the Bruggeman effective medium approximation (BEMA).[17] Four different BEMA models of increasing complexity and compatible with the oxide chemistry deduced by XPS analysis have been considered as shown schematically in Fig. 2. The reference data base provided by Theeten *et al.* have been used for the dielectric functions of *c*-GaAs, GaAs oxide, *a*-As, and voids. Once calculated, the BEMA results were compared with the experimental data using the unbiased estimator[15] χ^2 to evaluate the goodness of the fit from which film thickness and constituent volume fractions have been derived. The lower the χ^2 value, the better the fit.

III. RESULTS AND DISCUSSION

A. Oxidation kinetics

Figure 3 illustrates the typical (Ψ,Δ) ellipsometric trajectory recorded during the plasma oxidation of (100) GaAs at a

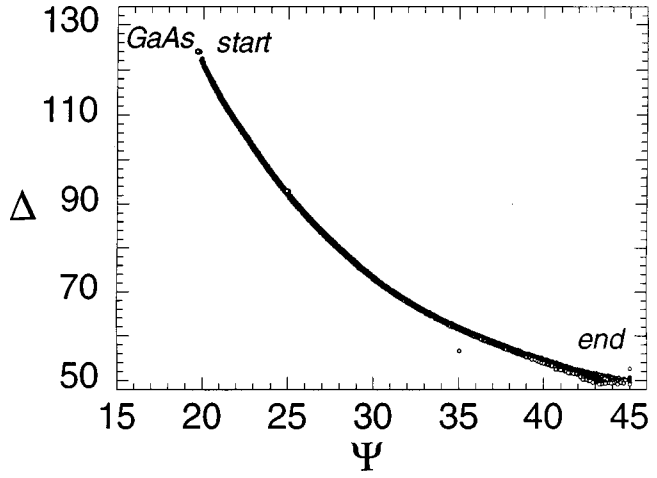

FIG. 3. (Ψ,Δ) trajectory at a photon energy of 3.45 eV recorded during the oxidation of (100) GaAs at $T = 130$ °C, rf power=100 W, $P = 0.1$ mbar, and bias voltage=+50 V. The total oxidation time is 230 min.

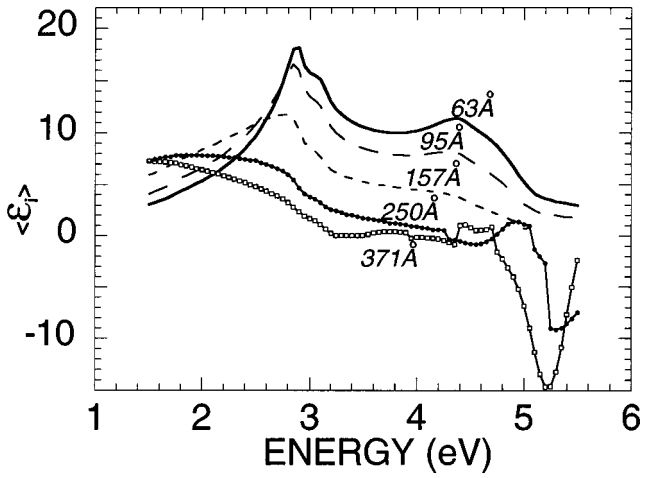

FIG. 4. Room-temperature spectra of the imaginary part of the pseudodielectric function $\langle \varepsilon_i \rangle$ of GaAs, recorded at different oxygen plasma exposure time during the oxidation experiment of Fig. 3.

surface temperature of 130 °C, a rf power of 100 W, a pressure of 0.1 mbar, and a bias voltage of +50 V. Starting from the upper-left point corresponding to a clean GaAs surface, the oxidation process induces a monotonic decrease in Δ and increase in Ψ. The plasma exposure was stopped at various times to perform SE measurements and the spectra of the imaginary parts of the pseudodielectric function, $\langle \varepsilon \rangle = \langle \varepsilon_r \rangle + i\langle \varepsilon_i \rangle$ corresponding to different oxide thicknesses are shown in Fig. 4. The two-layer optical model *D* provides the best fit for the spectra in Fig. 4. Thus, the experimental (Ψ, Δ) trajectory has been simulated by model *D* and transformed in the corresponding time dependence of the oxide thickness as shown in Fig. 5. In the same figure, the effect of the UV-light irradiation on the GaAs plasma oxidation kinetics is evidenced. At first sight, three different oxidation regimes can be distinguished in the kinetics without light irradiation: an *early oxidation regime* (EO regime) which corresponds to the very fast growth of 20–30 Å of oxides, a *transition regime* (TO regime) up to about 60 Å where the oxide thickness increases with the square root of time, as evidenced by the inset (a) of Fig. 5, and a *late oxidation regime* (LO regime) over 60 Å, where the oxide thickness increases linearly. Also in the UV case, the three different oxidation regime are present, but in the LO stage a photoenhancement of the oxidation rate is clearly seen. However, the UV photoeffect on the oxidation rate decreases with increasing the oxide thickness, and for oxide thicker than 250 Å, the photoenhancement effect disappears and the oxidation rate approaches the value measured without UV-light irradiation. This last result suggests that the UV photoeffect on the oxidation rate depends on the oxide layer thickness.

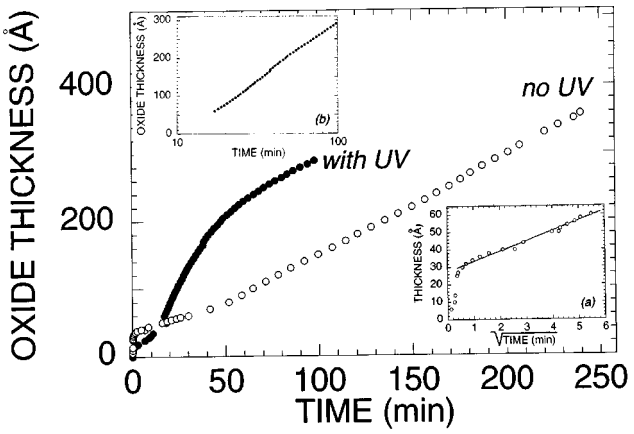

FIG. 5. Time evolution of the oxide thickness obtained during oxidation of GaAs with and without UV-light irradiation by an Hg arc lamp and at $T = 130$ °C, rf power = 100 W, $P = 0.1$ mbar, and bias voltage = +50 V. Inset (a) refers to data without UV-light irradiation and clearly evidences the EO regime and the square-root time dependence of oxide thickness in the TO regime defined in the text. Inset (b) refers to data with UV-light irradiation and evidences the logarithmic time dependence of oxide thickness in the LO regime.

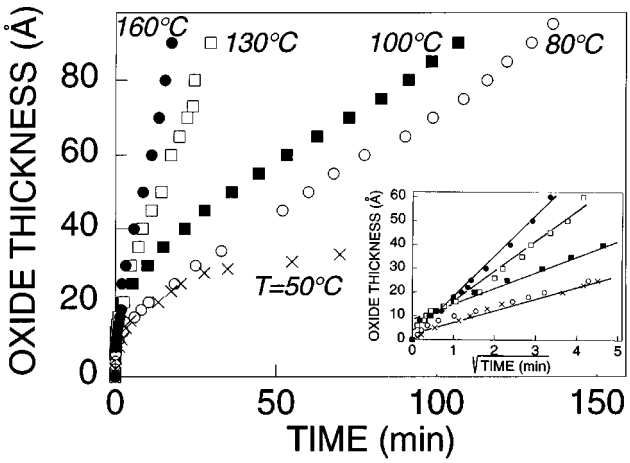

FIG. 6. Oxide thickness vs oxidation time at different temperatures of (100) GaAs surface. Other experimental conditions: rf power = 100 W, $P = 0.1$ mbar, and bias voltage = +50 V. The inset shows the square-root time dependence of oxide thickness.

The observed oxidation kinetics can be discussed on the basis of some general oxidation models described in literature, the most common being the linear-parabolic model (LP) developed by Deal and Grove[18] for the thermal oxidation of semiconductors (Si, Ge, etc.) and the Cabrera-Mott[19] (CM) model for oxidation by charged species of metals. When the LP model applies, a linear oxidation regime controlled by the semiconductor/oxygen reaction and a parabolic regime controlled by Fick's diffusion of oxidizing species are observed. Also, the oxide thickness depends on the square root of time when the CM model applies and the oxidation proceeds by migration of charged species in low-electric field. However, for plasma oxidation of Si, it has been demonstrated that when a positive bias voltage is applied to the semiconductor, the drift of ionic species in the electric field across the growing oxide layer is more important than diffusion and that none of the previous models are able to explain the early oxidation kinetics. Thus, additional models also predicting a linear-parabolic oxidation law have been formulated.[20,21] In these models, the oxidation kinetics depends on the thickness of the oxide layer itself, x, on the potential across the oxide layer V, on the temperature T, and on the diffusion coefficient D, i.e., $x = f(x, V, T, D)$.

Figure 6 shows that the dependence of oxide thickness on oxidation time for oxide grown in the temperature range 25–160 °C with a +50 V bias voltage. As expected, the oxidation rate increases with temperature, and the observed pro-

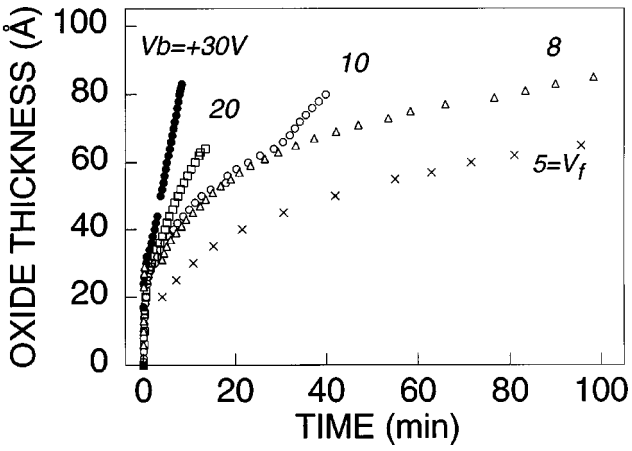

FIG. 7. Time evolution of oxide thickness at different bias voltage during UV-light photoassisted plasma oxidation of (100) GaAs surfaces. Other experimental conditions: rf power=100 W, P =0.1 mbar, and T=130 °C.

files in the TO regimes conform to a square-root time dependence as evidenced by the inset of Fig. 6. Moreover, it can be seen that the EO and TO regimes tend to collapse in a unique diffusive regime at high temperature.

As for the effect of bias voltage, the time evolution of the oxide thickness in the EO and TO regime for different bias voltage values is shown in Fig. 7. It is well evidenced that the EO regime is nearly bias independent while the time duration of the TO regime depends on bias voltage, i.e., the higher the bias, the shorter the TO regime. However, the time duration of the EO and TO regimes depends not only on the oxidation parameters but also on the history of the GaAs substrate and, in particular, on its surface morphology. In fact, different GaAs substrates, as derived by different cleaning treatments and, hence, with a different surface roughness and porosity [see SE spectra in Fig. 8(a)] have different oxidation kinetics as shown in Fig. 8(b). Here, it is evident that the higher the surface roughness, the faster the EO regime and that in the case of low-surface roughness (substrate *a*), the EO and TO collapse in a single diffusion regime again, as shown by the square-root-time plot in the inset.

At first sight, the data appear to give evidence that the oxidation of the outmost porous layer (10–30 Å) is an easy process occurring in a relatively short time of a few tens of seconds. In this EO stage, the GaAs is oxidized throughout its entire volume due to its open porosity and the easy diffusion of oxygen atoms into the pores.

Once a thin oxide layer has been grown and a uniform electric field applies across the oxide layer, the oxidation becomes field-aided, as evidenced by the bias dependence shown in Fig. 7. Thus, in the TO regime, the oxidation is determined by both in-diffusion of oxidizing species at plasma/oxide interface and out-migration of gallium and arsenic ionic species at the oxide/GaAs interface. As a consequence, the oxidation is not a surface process but takes place over a reaction volume zone whose extension depends on the competition between diffusion and ion drift, i.e., the higher the electric field, the more predominant is the ion drift and the shorter the TO regime (see Fig. 7).

Following the TO regime, the electric field in the oxide layer becomes uniform and well set, and the oxide growth is

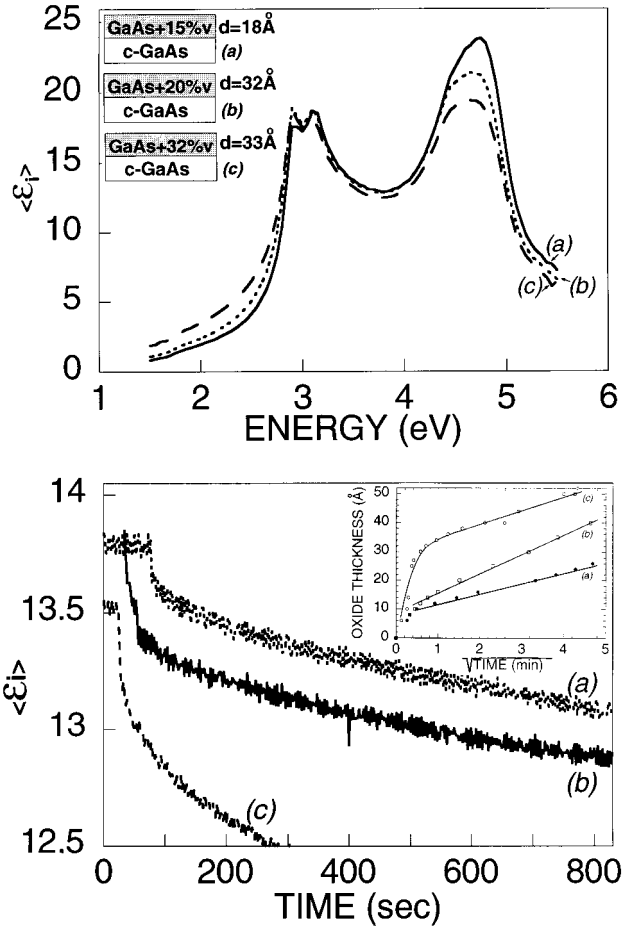

FIG. 8. $\langle \varepsilon_i \rangle$ decrease during the early oxidation regime for GaAs substrates treated by (a) wet etching with HCl/MeOH for 2 min, (b) hydrogen plasma at T=230 °C for 2 min, (c) hydrogen plasma at T=500 °C for 5 min. Other oxidation experimental conditions: rf power=100 W, P=0.1 mbar, T=130 °C, and bias voltage=+50 V.

controlled by drift of Ga and As ions towards the plasma/oxide interface, as already demonstrated by Yamasaki and Sugano.[8] In this LO regime, under almost constant anodization current, the oxide thickness x_{oxide} is approximately proportional to the oxidation time, i.e., x_{oxide}=kt as shown by data in Fig. 5. Obviously, an increase in bias voltage (or anodization current) results in an increase of oxidation rate. The linear dependence between oxidation rate and anodization current is evidenced by the data in Fig. 9, where both oxidation experiments with and without UV-light irradiation are considered. In the case where UV light irradiates the samples, the initial slope of the oxide thickness profile in the LO regime has been considered as a measure of the oxidation rate. Thus, according to the model of Yamasaki and Sugano, the oxidation rate, in the LO regime, is limited by the drift of Ga and As ions across the oxide for both oxidation processes occurring with and without UV-light irradiation.

The different kinetics observed in the oxidation with and without UV-light irradiation can provide more insight into the oxide growth mechanism. In particular, the fact that the oxidation rate photoenhancement is a function of the oxide thickness itself and that the photocatalytic effect disappears for thickness larger than 250 Å (see Fig. 5) can be explained

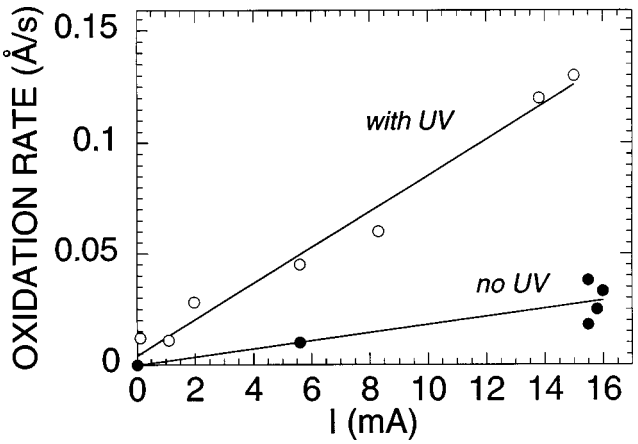

FIG. 9. Variation of initial oxidation rate in the LO regime (see text) as a function of current applied to GaAs samples for oxidation occurring with and without UV-light irradiation.

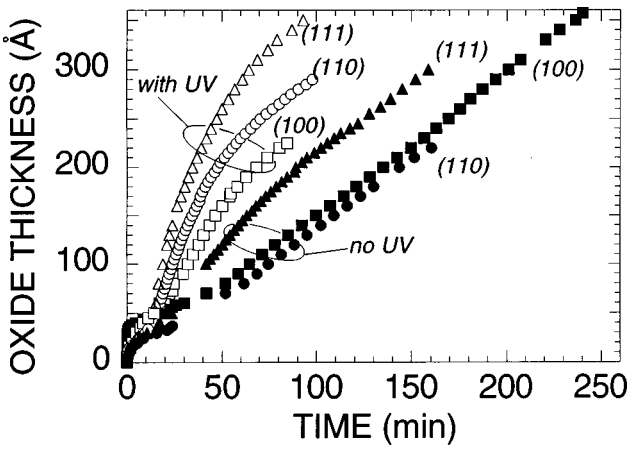

FIG. 10. Oxide thickness profile grown on GaAs wafers with (100), (110), and (111)*A* crystal orientations during plasma oxidation without and with UV-light irradiation, at a rf power of 100 W, a pressure of 0.1 mbar, a surface temperature of 130 °C, and a bias voltage of +50 V.

by considering that the UV light is increasingly absorbed by the oxide layer according to the Lambert-Beer law.

In fact, the oxidation rate in the LO regime is determined by the combination of two processes: one is the drift of Ga and As ions due to the electrical field at the oxide/GaAs interface, and the other is the photoenhancement of the oxidation rate caused by the UV-light irradiation of the GaAs surface. The combination of these processes can be represented by the following relation for the oxidation rate:

$$\frac{dx}{dt} = k(1 + \gamma I_o e^{-\alpha x}), \tag{1}$$

where k is the oxidation rate constant in the constant current mode (the anodization current remains constant during oxide growth), γ is the photocatalytic coefficient, I_o is the light intensity at the oxide surface, and α is the GaAs-oxide absorption coefficient.

For the sake of simplicity, let us assume two limiting cases. (a) Plasma oxidation occurs without light irradiation ($I_o = 0$), or with light irradiation but the grown oxide layer is thick enough to have large light absorption ($\gamma I_o e^{-\alpha x} \ll 1$). In these cases, the time dependence of the oxide thickness is of the type

$$x = k\ t. \tag{2}$$

(b) Plasma oxidation occurs with light irradiation and the oxide layer is thin enough to have light on the GaAs surface ($\gamma I_o e^{-\alpha x} \gg 1$). In this case, the time dependence of the oxide thickness is of the type

$$\alpha x = \ln t + \text{const}. \tag{3}$$

An excellent fit of the experimental data to Eq. (3) for the thin oxide film (<250 Å) is shown in inset (b) of Fig. 5. The slope of the straight line is a measure of the absorption coefficient α in the UV spectral region, of the grown oxide. As soon as the oxide thickness reaches 250 Å, the UV light is completely absorbed and the oxide growth proceeds with the linear dependence of Eq. (2) and at the same rate as without light irradiation.

The explanation of the photocatalytic effect can be found in the generation of Ga and As ions at the GaAs/oxide interface. In fact, UV photons reaching the GaAs surface can promote, among other photon-associated phenomena, internal photoemission and the GaAs ionization processes (GaAs photoelectron threshold energy ranging between 4.7–5.5 eV).[22] Therefore, the production of Ga and As ions is enhanced and, consequently, a higher oxidation rate is observed.

B. Crystal orientation effect

In the oxidation processes on semiconductor surfaces anisotropy effects have attracted considerable attention, i.e., the variation of oxidation rate on the different crystallographic surfaces of oriented materials. The anisotropy has been clearly demonstrated by Lewis and Irene,[23] particularly in relation to the thermal oxidation of Si system under both interface and diffusion controlled kinetics.

Figure 10 shows oxidation kinetics recorded during oxidation with and without UV-light irradiation of GaAs wafers having (100), (110), and (111)*A* crystal orientations. Apart from small differences observed in the EO regime due to the different surface morphologies, the oxidation kinetics without UV-light irradiation were found to be almost independent of the crystal orientation. This is expected since, as we have seen above, the oxidation rate in the LO regime is limited by the ion drift and not by surface reactions at the GaAs/oxide interface. The slightly faster kinetics observed for the (111)*A* orientation without UV-light irradiation is due, as will be shown below, to a higher sensitivity of this orientation to the UV light coming from the glow of the plasma which has not been screened. The absence of crystal orientation associated phenomena has also been found by Lefebre and Irene) in a very recent work[24] on the GaAs oxidation by ECR oxygen plasmas.

On the contrary, when plasma oxidation proceeds with UV-light irradiation by the Hg-arc lamp, the oxidation kinetics is clearly dependent on the crystal orientation as shown in Fig. 10, and the order of oxidation rate, r, is

$$r(111) > r(110) > r(100).$$

This anisotropic effect is similar to that reported by Lewis and Irene[23] for thermal oxidation of Si, over 10 nm of grown oxide; however, the oxidation is controlled by the reaction at the Si/SiO_2 interface. Also in the present case, the observed anisotropic effect can be explained by different interactions of the UV light with the three different GaAs surfaces at the oxide/GaAs interface. In fact, for the photoenhanced generation of Ga and As ions, two factors have to be considered: the surface density d of Ga and As bonds available for a particular crystal plane, being

$$d(110) > d(111) > d(100),$$

and the orientation dependence of the photoemission threshold energy E, which increases in the order[25]

$$E(111) = 4.7 \text{ eV} < E(100) = 5.1 \text{ eV} < E(110) = 5.5 \text{ eV}.$$

Thus, it seems that the significantly lower threshold energy for the (111) orientation enhances the GaAs ionization process, explaining the faster oxidation rate for (111) and the crossover in the order of the (110) and (111) orientations as expected on the basis of the surface density values.

C. Oxide chemistry

The joint XPS and SE analyses of the oxide chemistry have revealed that the composition of the oxide layers changes with the oxidation conditions and depends on the plasma parameters, the bias voltage, and UV-light irradiation. As for the overall stoichiometry, i.e., the Ga/As ratio, integrated intensities of Ga 3d and As 3d spectra at different take-off angles have been used for the semi-quantitative analysis of the oxide layers. It has been found that the Ga/As ratio is about 2 at the oxide surface and gradually decreases to a value of 1.2 in the oxide bulk, indicating a Ga enrichment in the outer oxide layers as already reported by many authors.[25,26]

The main feature of the plasma-grown oxides is the high As_2O_5/As_2O_3 ratio in comparison to that found in thermally grown GaAs oxide. The As_2O_5/As_2O_3 ratio is further enhanced by adding UV-light irradiation to plasma oxidation (see Fig. 11). The higher degree of arsenic oxidation observed under plasma anodization of GaAs, has been related to the charged oxygen species (O^-,O_2^-) (Ref. 25) whose chemisorption is further improved by UV-light irradiation. In addition, the As_2O_5/As_2O_3 ratio in the oxide bulk depends on the oxidation kinetics itself, as shown in Fig. 11: the slower the oxidation rate, the higher the As_2O_5/As_2O_3.

The oxidation rate also controls the chemical composition and width of the GaAs/oxide interface. Figure 12 shows some typical interfaces drawn on the basis of SE measurements and, for thinner samples, of angle-resolved XPS analysis. The feature is that by increasing the bias voltage and, hence, the oxidation rate, the layer containing free As becomes thicker and thicker but, at the same time, the free As becomes more diluted.

IV. CONCLUSIONS

We have shown the feasibility of evaluating both the chemistry and kinetics of the GaAs plasma oxidation process using real time *in situ* spectroscopic ellipsometry. The SE and the SWE traces have been examined on the basis of BEMA models whose applicability and validity, although widely demonstrated by many authors in the past, has been confirmed by XPS and atomic force microscopy measurements.

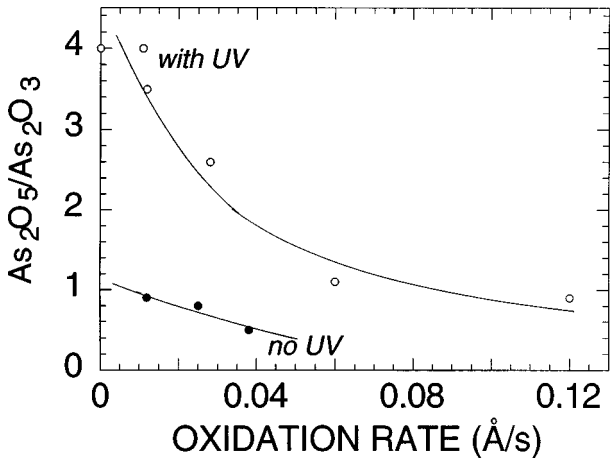

FIG. 11. As_2O_5/As_2O_3 ratio vs oxidation rate for oxide layer grown under UV-light irradiation and by changing the positive bias potential in the range 5–50 V. Other experimental conditions: rf power=100 W, $P=0.1$ mbar, $T=130$ °C.

The key points of the GaAs oxidation process to be understood refer to the quality (defect density) of the GaAs/oxide interface and, hence, to the early stage of oxidation ($\leqslant 200$ Å). The following facts summarize our results.

(i) Surface morphology and oxygen diffusion control the growth of the first 20–30 Å of oxide (*early oxidation regime*).

(ii) Oxygen diffusion and Ga and As ion drift concur in thickening the oxide up to 60 Å (*transition oxidation regime*).

(iii) Ga and As ion drift alone determines the oxide growth up to 350 Å in our *case* (*late oxidation regime*). Here, the oxidation rate is constant and its value increases linearly by increasing the bias voltage.

(iv) The oxidation kinetics are affected by irradiation of the surface with UV light. The photoenhancement of the oxidation rate, which becomes uneffective at oxide thickness of 250 Å has been assigned to a larger availability of Ga and As ions at oxide/GaAs interface due to the GaAs photoionization process.

(v) Depending on the GaAs crystal orientations, (100), (110), and (111)A, different oxidation kinetics are observed under UV-light irradiation.

(vi) A composition of the GaAs oxide layers is induced by plasma anodization and UV-light irradiation, in that these oxides are almost stoichiometric, i.e., Ga oxide to As oxide

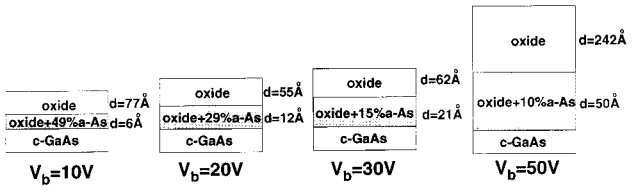

FIG. 12. Scheme of some typical GaAs oxide grown at different bias voltage and, hence, different oxidation rate, as deduced by BEMA modeling of SE spectra and XPS analysis.

ratio is equal to 1.2, and contains As_2O_5 as the main arsenic oxide.

Although the presence of free arsenic is confirmed in the plasma grown GaAs oxides, all experimental evidence clearly supports the premise that further improvement in a very thin GaAs oxide layer can be achieved by a careful control of the plasma oxidation process. It remains evident, however, that the definitive validation of the GaAs plasma oxidation process, under optimized conditions, can be settled by the performance of a metal-insulator-semiconductor device, which includes a GaAs oxide interlayer.

ACKNOWLEDGMENTS

The authors wish to express their thanks to Professor Eugene A. Irene of the University of North Carolina for the helpful discussion and critical reading of the manuscript.

[1] C. W. Wilmsen, R. W. Kee, and K. M. Geib, J. Vac. Sci. Technol. **16**, 1434 (1979).
[2] F. Schroder, W. Storm, M. Altebockwinkel, L. Wiedmann, and A. Benninghoven, J. Vac. Sci. Technol. B **10**, 1291 (1992).
[3] P. Schmuki, G. I. Sproudle, J. A. Bardwell, Z. H. Lu, and M. J. Graham, J. Appl. Phys. **79**, 7303 (1996).
[4] K. M. Geib and C. W. Wilmsen, J. Vac. Sci. Technol. **17**, 952 (1980).
[5] Z. Lu, M. T. Schmidt, D. V. Podlesnik, C. F. Yu, and R. M. Osgood, J. Chem. Phys. **93**, 795 (1990).
[6] C. F. Yu, D. V. Podlesnik, M. T. Schmidt, H. H. Gilgen, and R. M. Osgood, Chem. Phys. Lett. **130**, 301 (1986).
[7] C. F. Yu, M. T. Schmidt, D. V. Podlesnik, E. S. Yang, and R. M. Osgood, J. Vac. Sci. Technol. A **6**, 754 (1988).
[8] K. Yamasaki and T. Sugano, J. Vac. Sci. Technol. **17**, 959 (1980).
[9] F. Koshiga and T. Sugano, Thin Solid Films **56**, 39 (1979).
[10] R. P. H. Chang, Thin Solid Films **56**, 89 (1979).
[11] R. P. H. Chang, A. J. Polak, D. L. Allara, and C. C. Chang, J. Vac. Sci. Technol. **16**, 888 (1979).
[12] C. C. Chang, R. P. H. Chang, and S. P. Murarka, J. Electrochem. Soc. **125**, 481 (1978).
[13] J. B. Theeten, R. P. H. Chang, D. E. Aspnes, and T. E. Adams, J. Electrochem. Soc. **127**, 378 (1980).
[14] G. Bruno, M. Losurdo, and P. Capezzuto, J. Vac. Sci. Technol. A **13**, 349 (1995).
[15] G. Bruno, P. Capezzuto, and M. Losurdo, Phys. Rev. B **54**, 17 175 (1996).
[16] Y. L. Chang, R. Cao, W. E. Spicer, P. Pianetta, S. Shi, and E. Hu, J. Vac. Sci. Technol. B **14**, 2914 (1996).
[17] D. A. G. Bruggemann, Ann. Phys. (Leipzig) **24**, 636 (1935).
[18] B. E. Deal and A. S. Grove, J. Appl. Phys. **36**, 3770 (1965).
[19] N. Cabrera and N. F. Mott, Rep. Prog. Phys. **12**, 163 (1948).
[20] Y. Z. Hu, Y. Q. Wang, M. Li, J. Joseph, and E. A. Irene, J. Vac. Sci. Technol. A **11**, 900 (1993).
[21] Y. Wang, Y. Z. Hu, and E. A. Irene, J. Vac. Sci. Technol. B **14**, 1687 (1996).
[22] O. Madelung, *Semiconductors: Physics of Group IV Elements and III-V Compounds*, Landolt-Bernstein, New Series, Group X, Vol. 17 (Springer-Verlag, New York, 1982).
[23] E. A. Lewis and E. A. Irene, J. Electrochem. Soc. **134**, 2332 (1987).
[24] P. R. Lefebvre and E. A. Irene (unpublished).
[25] G. Hollinger, R. Skheyta-Kabbani, and M. Gendry, Phys. Rev. B **49**, 11 159 (1988).
[26] C. W. Wilmsen, *Physics and Chemistry of III-V Compound Semiconductor Interfaces* (Plenum Press, New York, 1985), p. 403.